

AD-A266 293



Technical Document 2461
March 1993

Porous Silicon For Pumping Solid-State Lasers

S. D. Russell
W. B. Dubbelday
R. L. Shimabukuro

DTIC
ELECTE
JUN 29 1993
S B D

Approved for public release; distribution is unlimited.

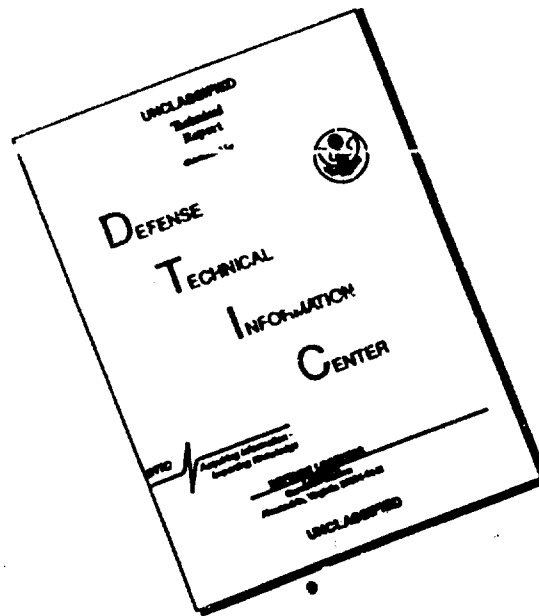


93-14885



93 6 99 10 5

DISCLAIMER NOTICE



THIS DOCUMENT IS BEST QUALITY AVAILABLE. THE COPY FURNISHED TO DTIC CONTAINED A SIGNIFICANT NUMBER OF PAGES WHICH DO NOT REPRODUCE LEGIBLY.

Technical Document 2461
March 1993

Porous Silicon For Pumping Solid-State Lasers

S. D. Russell
W. B. Dubbelday
R. L. Shimabukuro

**NAVAL COMMAND, CONTROL AND
OCEAN SURVEILLANCE CENTER
RDT&E DIVISION
San Diego, California 92152-5001**

J. D. FONTANA, CAPT, USN
Commanding Officer

R. T. SHEARER
Executive Director

ADMINISTRATIVE INFORMATION

The research presented in this work was funded by the Office of Naval Research, Solid-State Laser (6.1.5) block program and in part by the NCCOSC, RDT&E Division Independent Research (IR) program.

Released by
G. A. Garcia, Head
Research and Technology
Branch

Under authority of
H. E. Rast
Solid State Electronics
Division

ACKNOWLEDGMENTS

The authors thank Dr. F. Hanson (NRaD, Code 843) and Dr. M. Sailor (Dept. of Chemistry, UCSD) for making their labs available for the collection of photoemission spectra, and S. Pappert (NRaD, Code 555) for supplying the multiple quantum well Al-GaAs/GaAs sample used in this investigation. The authors also thank D. Gookin (NRaD, Code 843) for exchanging information concerning a novel application for porous silicon, and Dr. V. Smiley (NRaD, Code 804) and Dr. A. Gordon (NRaD, Code 0014) for funding this research. Finally, the authors thank Dr. D. Szaflarski (ONT/ASEE postdoctoral fellow, now at Molecular Biosystems) and P. Georgief (SDSU Foundation Student) for preparing some of the samples used in this work.

CONTENTS

BACKGROUND	1
DIODE-PUMPED SOLID-STATE LASERS	1
POROUS SILICON	3
OBJECTIVE	4
APPROACH	4
DELIVERABLES	4
PERIOD OF PERFORMANCE	4
EXPERIMENTAL RESULTS	4
POROUS SILICON FABRICATION PROCESS	4
POROUS SILICON ON SAPPHIRE	5
QUANTUM EFFICIENCY OF POROUS SILICON	7
RECENT RESULTS	10
FUTURE DEVELOPMENTS	10
CONCLUSIONS	11
REFERENCES	11
 FIGURES	
1. Common energy levels for solid-state lasers.	2
2. Silicon band structure.	3
3. Photoluminescence spectra of porous SOS.	6
4. SEM cross section of porous SOS.	7
5. Diode laser and porous silicon emission spectra.	8
6. MQW and porous silicon emission spectra.	9

DO NOT WRITE IN THESE SPACES

Accession For	
NTIS - TAB1	<input checked="" type="checkbox"/>
DTIC TAB	<input type="checkbox"/>
Unannounced	<input type="checkbox"/>
Justification	
By _____	
Distribution/	
Availability Codes	
Dist.	Avail and/or Special
A-1	

BACKGROUND

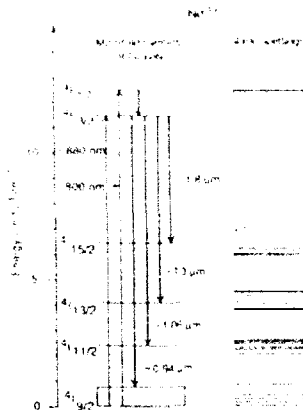
DIODE-PUMPED SOLID-STATE LASERS

Solid-state lasers have military, scientific, and commercial applications in, for example, ranging, imaging, spectroscopy, nonlinear optics, and materials processing. Diode laser pumping offers an all-solid-state laser with high efficiency in a simpler, more reliable, and compact system. These systems offer many improvements over the use of diode lasers themselves, including narrower frequency linewidth, better beam quality, higher peak powers, and different wavelengths. Diode lasers are attractive as pumps because they are compact, efficient, and reliable. However, since they are fabricated from III-V compound semiconductors, they are expensive. The emission wavelengths of diode lasers may be adjusted by varying the material composition during wafer growth and precisely matched to coincide to peak absorption lines by controlling the operating temperature. Therefore, diode pumps cause less undesirable heating and produce no damage such as may occur when high-energy photons from flashlamps are present in the pump light. In addition, because the diode pumps are partially coherent devices, the output beams may be efficiently focused and optically coupled to spatially match the solid-state laser mode.

Solid-state lasers operate in various manners and configurations, and virtually all of these lend themselves to the use of diode pumps. The geometrical configurations include a rigid cylindrical rod, a slab, and a flexible optical fiber. Solid-state lasers operate in CW, long-pulse (μs time frame) and short-pulse (Q-switched) forms. The emission may contain single or multiple spatial or longitudinal modes. The use of diode pumps provides for several new pump-resonator configurations; for example, transversely pumped rod or slab systems for pulsed high-power multimode output, analogous to flashlamp-pumped systems; longitudinally CW end-pumped rod systems for low-power output with high efficiency because of the ability for optical mode matching in the lasing volume; and longitudinally pumped scalable slab or disc systems for high CW power in the fundamental (TEM_{00}) mode by increasing both the radial and longitudinal component of the pumped volume [1].

Diodes fabricated from AlGaAs with different concentrations of Al and Ga emit at wavelengths of about 800 nm, ranging from about 700 to 900 nm. These emission wavelengths coincide well with the strong absorption bands of several currently important solid-state lasing ions, including, for example, neodymium, holmium, erbium, and promethium. Typical pumping requirements at the desired wavelength are tens of milliwatts to hundreds of milliwatts. Threshold pumping values of 6–12 mW for Nd:NPP ($\text{Nd:P}_5\text{O}_{14}$) and LNP ($\text{LiNdP}_4\text{O}_{12}$) with reasonable efficiency have been reported [2]. Laser emission has also been reported from Ho:YAG at 2.1 μm , Er^{3+} :YLF at 2.8 μm , Nd:YAG at 0.946 μm , Nd:YVO₄ at 1.06 μm , and Nd:glass at 1.06 μm ; these and others have been thoroughly reviewed in the scientific literature [1–4]. Figure 1 describes some common energy level schemes for solid-state lasing, and the desired pump wavelengths [2]. This shows that pump sources emitting between 700 and 900 nm may be employed to pump a large variety of laser hosts. Additional information can be obtained from Kaminskii [4]. The host crystal for these lasing ions plays a role in the fine structure of the absorption bands due to the Stark splitting by the crystal field, but does not substantially

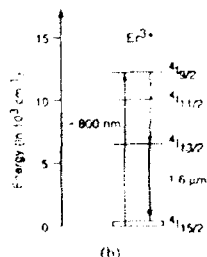
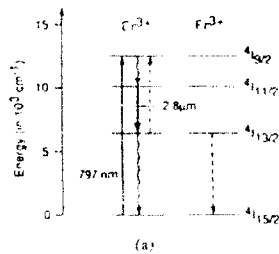
change the required spectral region required for the efficient pumping of the ions into the excited states desired for laser emission. For reference, the best optical efficiency in diode-pumped solid-state lasers is 19% (Nd:YAG) [3] compared to 8% efficiency in a flashlamp-pumped coaxially cylindrical Nd:glass rod, although more typically it is 5% with a flashlamp with Nd,Cr:GSGG or Er, Tm, Ho:YAG [2]. Therefore, research into high-efficiency pumping schemes is ongoing.



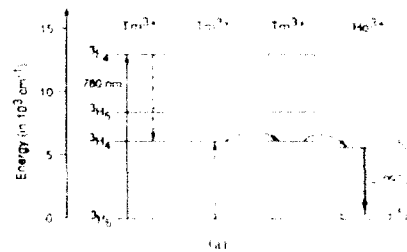
Energy level diagram of Nd^{3+} . The laser transitions are shown in heavy lines, diode pump transitions in light lines, and relaxation in wavy lines. The first proposed diode-pumped laser transition was ${}^4F_{3/2} \rightarrow {}^4I_{11/2}$ near $1.06 \mu m$ pumped at $880 nm$. Representative Stark splittings of the manifolds are shown on the right hand side. The actual laser transitions occur between these individual Stark splittings. The open box for the ground-state manifold indicates that the laser transition to this manifold is to an energy level above the ground state.



Energy level schemes of diode-pumped solid state lasers: (a) Yb^{3+} :YAG, (b) Tm, Ho:LuYbF₆. Arrows between ions indicate energy transfer.



Energy level schemes in Er^{3+} : (a) ${}^4I_{11/2} \rightarrow {}^4I_{13/2}$, (b) ${}^4I_{13/2} \rightarrow {}^4I_{15/2}$. Dashed lines in (a) indicate upconversion.



Energy level schemes in recently demonstrated diode-pumped solid state lasers: (a) Tm³⁺, Ho³⁺:YAG and (b) Tm³⁺:YAG at $2.3 \mu m$ with a possible transition at $1.5 \mu m$ also illustrated.

Figure 1. Common energy levels for solid-state lasers. (From [2].)

POROUS SILICON

Figure 2 shows the band structure for single crystal silicon [5]. Since the conduction band minimum does not have the same crystal momentum (\mathbf{k}) as the valence band maximum, the band gap (denoted by E_g) is an indirect gap. In silicon, radiative recombination can only take place with the assistance of a phonon, making such transitions inefficient. This has prevented silicon from being used as a solid-state source of light, unlike group III-V semiconductors, which have a direct gap at the center of the Brillouin zone ($\Gamma = 0$). The discovery of photoluminescence in porous silicon has therefore generated a new optoelectronic material for study [6]. The typical emission spectrum of electrochemically etched porous silicon is in the red, orange, and yellow region (nominally 500 to 750 nm), although green and blue emissions have also been demonstrated. A blue shift of the peak emission wavelength has been shown by increased oxidation and etching of porous silicon [7] and by photochemical etching under illumination with high-energy photons*. At this time, the light-emitting mechanism is not well understood, with three competing theories existing: quantum size effects [6,7], amorphous silicon radiative emission [8], and surface passivation species that allow molecular radiative species that allow molecular radiative emission [9,10]. The fabrication processes must be examined to elucidate the mechanism with a view toward engineering the desired emission wavelength for solid-state laser pumping applications.

Recent research has suggested the potential of devices fabricated from porous silicon. The photoemission from porous silicon was reported to exhibit an integrated intensity three times greater than that of a commercial (AlGa)As LED [11]. This offers hope for an efficient light-emitting device that is competitive with III-V compound semiconductor devices. The demonstration of electroluminescence from porous silicon [12] was a key step in obtaining useful optoelectronic devices. The implication of this milestone is that the scalability and large-scale integration achievable in silicon microelectronics may be exploited in the fabrication of arrays of light-emitting structures. This may lead to practical devices such as LEDs, superluminescent diodes, or even silicon-based lasers (which may be achievable with further development).

Preliminary experiments at NReD's Microelectronics Laboratory have demonstrated photoluminescence in both bulk silicon and silicon-on-sapphire (SOS) prepared by chemical, photochemical, and electrochemical techniques [13]. Porous silicon on a transparent substrate (sapphire) presents advantages both for materials studies and possible device applications, since the emission can be observed through the substrate, which may enable more efficient pumping of solid-state laser host materials.

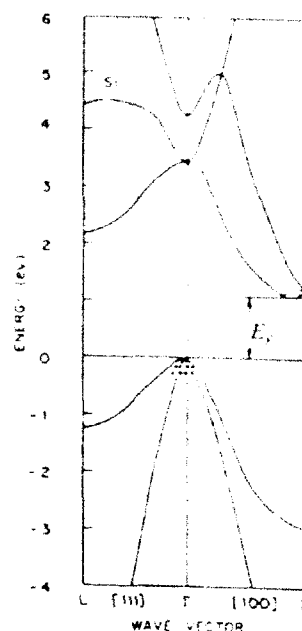


Figure 2. Silicon band structure.

* Private communication from M. J. Sailor, Dept. of Chemistry, University of California, San Diego (UCSD).

OBJECTIVE

The objective of this research is to perform preliminary experiments to examine the feasibility of using porous silicon and related devices for pumping solid-state lasers.

APPROACH

The controlled fabrication of light-emitting silicon structures will be developed using chemical, electrochemical, or photochemical techniques. Emphasis will be placed on techniques compatible with the requirements for the VLSI device processing of wafer size and etching uniformity. The optical and microstructural properties will be characterized using in-house facilities. This will elucidate the emission mechanism, which may allow the required engineering of the emission wavelength peak. In addition, variations in processing conditions and in silicon film thickness on sapphire will be examined for more precise control of the porous silicon thickness. These methods may provide the means to control the peak wavelength of the emission and may also allow control of the emitted linewidth. The photoluminescence intensity from porous silicon will be quantitatively measured for comparison with competing semiconductor pump sources.

DELIVERABLES

A preliminary report summarizing the experiments performed and conclusions was submitted 30 September 1992. The current technical document is the final deliverable and will complete this preliminary study of the feasibility of using porous silicon as a solid-state laser pump source.

PERIOD OF PERFORMANCE

The period of performance for this work was 1 June 1992 to 30 September 1992.

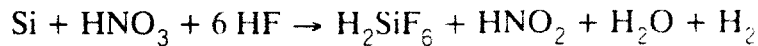
EXPERIMENTAL RESULTS

POROUS SILICON FABRICATION PROCESS

Porous silicon is commonly fabricated by the anodic oxidation of silicon in hydrofluoric acid (HF) solutions [6,7,8–11]. A solution of equal parts of HF and ethanol is typically used in a conventional electrochemical cell, with a platinum cathode and the silicon forming the anode. Current densities from about 1 to 100 mA are passed through the solution, causing the dissolution of the silicon and the creation of a physically porous structure with a reduction in density. This technique was used in this work to fabricate thick porous silicon films on bulk silicon, where it is simple to apply electrical contact to the backside of the sample (wafer). But this technique is less valuable in the fabrication of porous silicon films on sapphire due to the electrical insulation ($> 10^6 \Omega$ – cm resistivity) of the substrate. In addition, the requirement of obtaining highly uniform porous regions for future device applications suggests that an

investigation be conducted of fabrication techniques more compatible with conventional VLSI processing. In this work, we demonstrated the first photochemical fabrication of porous silicon, and also investigated chemical stain etches reported in the literature [14,15] as requiring no electrical current.

The chemical stain etch used a solution of HF:HNO₃:deionized H₂O (1:5:10). Bulk silicon and SOS wafers were similarly processed. The bulk wafers were (100)-oriented B-doped silicon with 3–5 Ω-cm resistivity. The SOS samples were epitaxially deposited silicon, boron-doped in situ to 4 × 10¹⁵ cm⁻³, on 270-nm-thick SOS (1 × 10¹⁸ cm⁻³) to a total silicon thickness of 10 μm. The etch solutions were prepared by reacting a square centimeter of silicon with the HF:HNO₃ mixture for 2 minutes, causing an accumulation of HNO₂, the active oxidizer in the reaction [17]. The chemical etch is a result of hole injection from the HNO₃ oxidant into the silicon substrate via the following net reaction [16]:



The reaction is catalyzed by the presence of NO₂⁻ ions, and so there is usually an induction period observed for the etching process. Deionized H₂O was subsequently added to the solution before the sample to be etched was immersed. Typical etch times ranged from 1 to 15 minutes. The samples were rinsed with deionized water, dried with nitrogen, and examined with a hand-held ultraviolet lamp (Mineralight Model #S52). Generally, samples etched for less than 1 minute did not luminesce, whereas SOS samples that are etched longer than ~ 15 minutes resulted in the complete dissolution of the silicon off the sapphire substrate.

We also demonstrated for the first time that photoluminescent porous silicon is produced via a photoinitiated chemical stain etch. For these experiments, (100)-oriented bulk silicon, ⁷⁵As-doped to 1–1.8 Ω-cm, were used. The n-type SOS samples were epitaxially deposited silicon, phosphorous-doped in situ (10¹⁵ cm⁻³), on 270-nm-thick SOS (⁷⁵As-doped to 10¹⁸ cm⁻³) to a total silicon thickness of 10 μm. The acid mixture of HF:HNO₃ was diluted with distilled H₂O (same ratios as above) and placed in optical quality cuvettes. The samples were immersed in solution and illuminated for 2–10 minutes using a 5-mW HeNe laser. For short times, typically 1-minute etching occurs only in the regions where the sample is illuminated. Patterns generated by double-slit diffraction produced distinguishable etched features of about 30 μm with both the bulk and SOS materials. As the illumination time increased, the etching spread out to regions of the silicon which were not illuminated and small etched features became washed out, which is consistent with the generation of holes required for the catalysis of the etching mechanism described above. After the samples were rinsed with deionized H₂O and dried with nitrogen, they displayed visible orange photoluminescence upon UV illumination. The porous silicon layer thickness was found by using scanning electron microscopy (SEM) to be ~ 300 nm for samples irradiated 8 minutes.

POROUS SILICON ON SAPPHIRE

The photoluminescence spectra of etched samples were obtained using a defocused (5 mW/cm²) 442-nm HeCd laser for excitation, and the emission was collected by a 0.25-m monochromator with CCD detector. The collection spot size was about 1 mm in diameter.

Care was taken to record the emission spectra within five minutes of sample preparation in order to minimize the degradation of the luminescence, which in some cases is observed with exposure to air. The porous SOS samples show photoluminescence signals comparable to those published for p-type bulk silicon [14,15]. The photoluminescence spectra of 10- μm -thick SOS etched for 9 minutes are shown in figure 3. The two curves shown are the emission spectra obtained when the sample was illuminated and emission was collected at the silicon side (dotted line) and at the sapphire side (solid line) of the wafer. The photoluminescence maximizes in intensity at ~ 700 nm with a width of ~ 100 nm. The luminescence from the Cr^{+3} impurity (695 nm) is pronounced in the sapphire-side illumination spectrum. The similarity in the front and backside spectra suggests that there is uniformity in the porous structure with depth and that strain effects due to the lattice mismatch between the silicon and the sapphire are minimal.

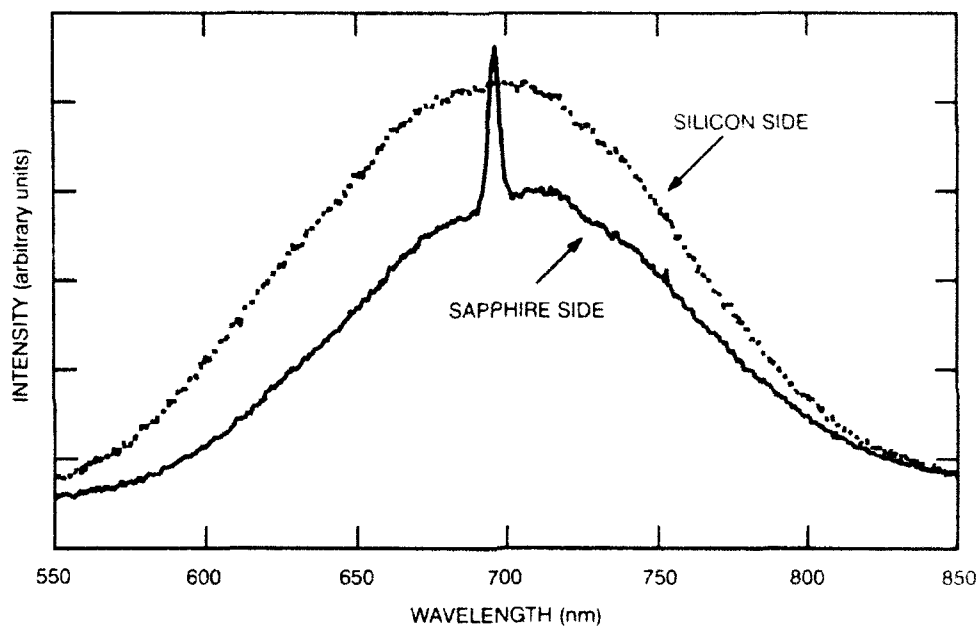


Figure 3. Photoluminescence spectra of porous SOS.

Fabricating porous SOS allows for the accurate control of the depth of the porous layer. Etching completely through the silicon layer to the silicon-sapphire interface allows control of the porous layer thickness by controlling the thickness of the silicon. The latter is controlled via either deposition techniques or oxidation/etch thinning processes, which are well-established VLSI techniques. Experiments on 0.3- μm -thick and 10- μm -thick SOS showed no significant difference in the photoluminescence characteristics of peak emission wavelength or linewidth. The thicker porous layer did exhibit an increased luminescence intensity relative to the thinner porous layer, which is attributed to the volumetric increase in the number of silicon emitters.

Identically processed bulk porous silicon and porous SOS exhibit qualitatively different emission when illuminated with a UV lamp. Bulk porous silicon, chemically etched as described above, emits a vivid luminescence, whereas the 10- μm -thick porous SOS sample exhibits a hazy, diffuse luminescence emission. In order to understand these differences, the

morphology of the samples was analyzed by using SEM. The thickness of the porous layer in the bulk porous silicon is about 100 nm, with a surface roughness of 10–20 nm. The porous layer on the SOS sample is less discernible, but shows a comparable surface roughness as shown in the SEM cross section in figure 4. Readily observable are additional crevices and cracks extending through the entire 10- μm silicon layer on sapphire. These cracks are attributed to preferential etching along threading dislocations and presumably cause diffuse scattering of the emitted photoluminescence. The dislocations arise from the thermal mismatch between silicon and the sapphire substrate which produces compressive stress in the silicon layer during the deposition at high temperature and subsequent cooling. This stress is partially relieved by the generation of threading dislocations. This hypothesis was examined by using Raman spectroscopy to measure the strain-induced splitting and shift in the $\text{O}(\Gamma)$ phonon. The resulting spectra from thick and thin film porous SOS exhibit a peak at $522.2 \pm 0.7 \text{ cm}^{-1}$, which is consistent with the relaxation of stress in the etched porous silicon film [13].

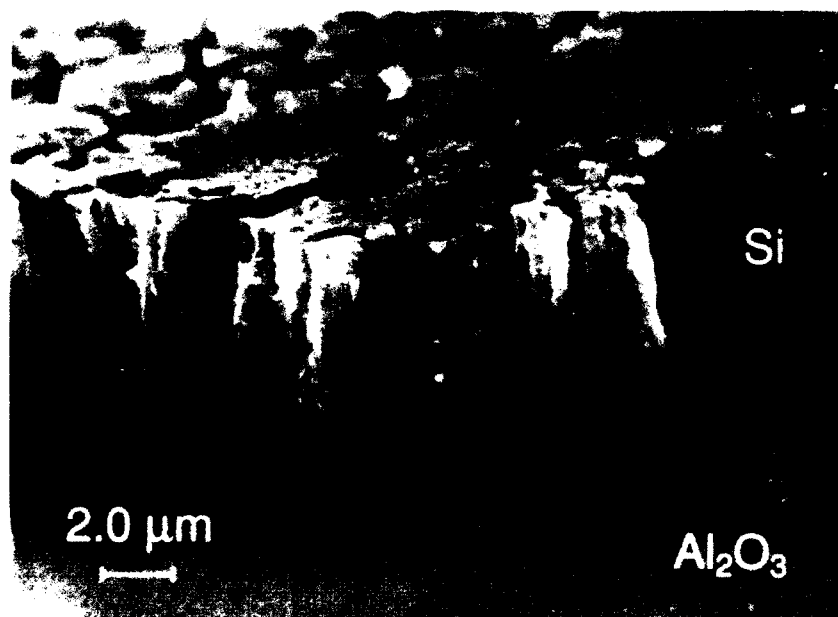


Figure 4. SEM cross section of porous SOS.

QUANTUM EFFICIENCY OF POROUS SILICON

Initial experiments into the quantum efficiency of porous silicon with respect to III-V compound semiconductors were performed by comparing the photoluminescence of undoped bulk-GaAs and 100- \AA -period multiple quantum well (MQW) AlGaAs/GaAs samples to an electrochemically prepared porous silicon sample. The electrochemically prepared porous layers could be fabricated several microns in depth in bulk silicon, and did not exhibit the diffuse scattering observed in the thick film porous SOS samples. Experiments were performed under 5-mW excitation, with the 457.9-nm line of an argon ion laser, and emission was detected by an Aires FF500MS monochromator with a silicon photodetector. No room

temperature photoluminescence was observed from the undoped bulk-GaAs sample, while the MQW-AlGaAs/GaAs sample exhibited a very weak room temperature photoluminescence, with some structure barely observable in the spectra. Under identical conditions, an electrochemically etched porous silicon sample exhibited strong photoluminescence at room temperature, with the peak wavelength at about 720 nm. The significant increase in light emission from the porous silicon sample compared to the MQW-AlGaAs/GaAs sample was clearly observable with the naked eye; however, in this experiment a quantitative comparison was not possible due to our inability to substantially detect photoluminescence from the III-V semiconductors at room temperature.

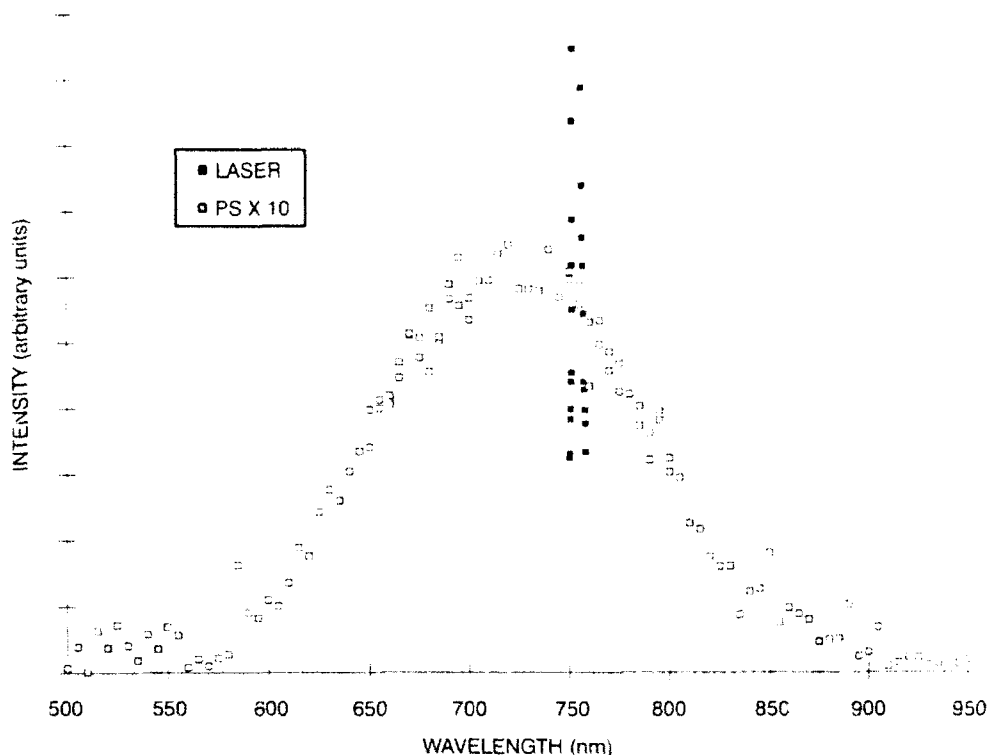


Figure 5. Diode laser and porous silicon emission spectra.

The emission spectra obtained for the porous silicon above were then compared to the emission from a commercial AlGaAs semiconductor laser (D.O. Industries GALA laser, model 975-04-8) under an identical light-collection arrangement. The intensity of the semiconductor laser was specified as 5 mW, with a peak wavelength about 755 nm. The integrated area was calculated for the two spectra, shown in figure 5, and corrected for geometrical factors. The integrated area for the semiconductor laser was 20 times that of our porous silicon sample, implying an emission of 0.25 mW. From these results, an external quantum efficiency of 5% was obtained.

Subsequent experiments were performed using a 10-mW HeCd laser (Liconix model 4210NB) at 442 nm. Emission spectra were collected by using a 0.25-m monochromator (Acton model 275, 150 grooves/mm grating) and a liquid-nitrogen-cooled CCD detector (Princeton Instruments). This experimental arrangement allowed for a substantially improved detection

of low light level due to the multichannel collection ability and the low dark current detector. Typically, 5 accumulations of 1-second exposures were used to obtain the emission spectra. Several of the electrochemically etched porous silicon samples were measured, with peak wavelengths ranging from 706 nm to 735 nm. All showed the characteristic broadband emission (~ 150 nm full width, half maximum) and had comparable relative intensities. The laser intensity was monitored during collection and the spectra were normalized to the maximum laser intensity when appropriate. The undoped GaAs sample was reexamined for room temperature photoluminescence. As many as 10 accumulations of 10 second exposures were acquired without evidence of photoemission. The MQW-AlGaAs/GaAs sample was also reinvestigated. The emission spectra were easily detected, with a peak about 843 nm. Figure 6 compares the photoluminescence emission spectra of the MQW and porous silicon. The commercial semiconductor laser was again used to quantify the magnitude of the photoluminescence. Correcting the data for geometrical aspects, we find that the integrated intensity of the porous silicon is greater than 10^3 times that of the MQW structure. In one region of interest, 750 nm to 900 nm, the room temperature photoluminescence of porous silicon exceeds that of the MQW sample by a factor of ~ 200 . Of course, the MQW has a much smaller linewidth and can be made to lase but for pumping applications the additional emission would be readily traded for linewidth. The emitted intensity from the "brightest" porous silicon sample was calculated to be $2.6 \mu\text{W}$. This corresponds to an external quantum efficiency of about 0.04%, substantially below that measured previously.

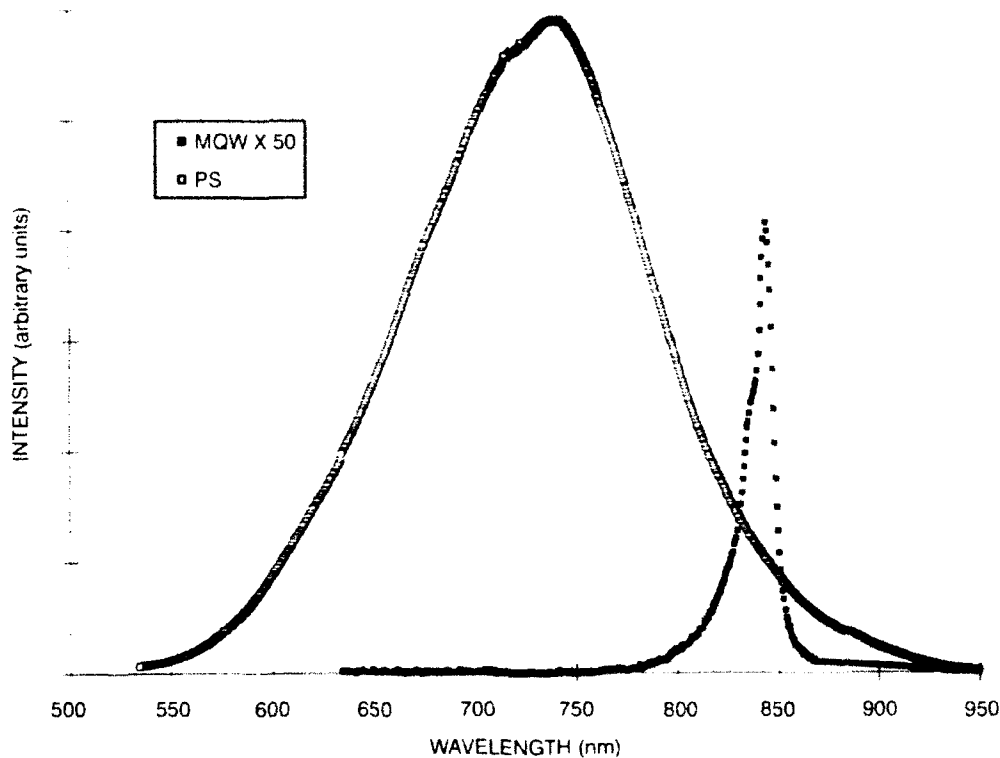


Figure 6. MQW and porous silicon emission spectra.

The shift to a shorter wavelength to photoexcite the samples would not be expected to cause the lower measurement for the quantum efficiency. In fact, the increased photon energy should photoexcite a larger population of states in the porous silicon, resulting in increased photoluminescence. The lower emission observed in this work from samples analyzed roughly 1 month apart is attributed to an aging effect observed in porous silicon. It has been reported [17,18] and has been observed here that oxidation of the samples occurs with prolonged exposure to air, which can be accelerated by illumination. This is evident by an increase in the Si-O peak in the FTIR spectra with time. We hypothesize that the oxidation process replaces surface hydrogens with oxygens and subsequently quenches the radiative emission. Investigation of this theory is ongoing.

RECENT RESULTS

Namavar et al. [19] of Spire Corporation report that the photoluminescence of their electrochemically prepared porous silicon samples emit intensities "essentially equal to those routinely found at Spire for MOCVD-grown $\text{Al}_{0.3}\text{Ga}_{0.7}\text{As}$ " and that the emission wavelength can be red-shifted by increasing the concentration of germanium in porous $\text{Si}_{1-x}\text{Ge}_x$ alloys. Electroluminescence was obtained from an n-ITO/p-PS-junction diode when forward biased. Correcting for series resistance, Namavar et al. project that the device would emit light with less than 3 volts applied.

At the fall 1992 Materials Research Society (MRS) conference,* there were several presentations of interest. Liu et al. (Stanford) reported on lithographically defined quantum pillars fabricated in bulk Si. This group has reported light emission from these pillars when substantial laser pumping (several W/cm^2) is used, and attempts are now underway to make contact with these nanostructures to investigate electroluminescence. Kozłowski et al. (Inst. Solid State Tech., Germany) reported electroluminescence at 5 volts in photoelectrochemically etched porous pn-junctions. Light emission from the blue to the red region of the spectrum was observed and could be tuned by varying the wavelength of incident light during the etching process. Maruska et al. (Spire Corp.) reported red electroluminescence and the first monolithic fabrication of a silicon light source (ITO/porous Si) and a silicon detector (ITO/Si). Peng et al. (Rochester) reported a means to passivate the porous silicon surface to prevent the degradation of photoluminescence by postfabrication etching in a nitric acid solution.

FUTURE DEVELOPMENTS

The investigation of the fundamental light emission mechanism in porous silicon and porous SOS and the development of fabrication techniques that are reproducible and compatible with microelectronic (VLSI) processing will be continued under the OCNR Independent Research (IR) program at NCCOSC, RDT&E Division during FY93. Advances from this program will be applicable to electroluminescent silicon and the further development of an efficient light-emitting silicon source.

* The presentations mentioned in this paragraph and related articles are published in the *Microcrystalline Semiconductor: Materials Science & Devices*, Vol. 283, Materials Research Society Symposium Proceedings, 1993.

CONCLUSIONS

Photoluminescent porous silicon and porous SOS have been fabricated by using chemical, electrochemical, and photochemical techniques. An electrochemically fabricated porous silicon sample exhibited 5% quantum efficiency when pumped with 5 mW of 457.9-nm argon ion laser light with a peak emission wavelength of 720 nm. This is consistent with other reports that efficiencies between 1 and 10% have been observed. This room temperature performance exceeds the early development of light emission from III-V semiconductors and suggests that continued research and development of the emission mechanism and optimization of the fabrication process can produce at least functionally equivalent results in a less expensive material which is amenable to large-scale integration.

In 1966, the external quantum efficiency of direct-band gap GaAs light-emitting diodes was reported greater than 1% [20]. The first diode laser-pumped solid-state ($\text{CaF}_2:\text{U}^{3+}$) laser demonstrated in 1962 required the entire assembly to be placed in a liquid helium dewar due to the requirements for the GaAs diode laser operation. Since then, a 100-mW AlGaAs diode array was commercially produced in 1984, and subsequently the output power has increased two orders of magnitude to 10 watts in multistriple bar arrays commercially available [2,3]. Extrapolation of similar rapid development can be made for porous silicon due to the mature silicon processing infrastructure in-place worldwide. This is evident by the monolithically integrated silicon-based source and detector and the rapid advances in silicon LEDs. Improvements in fabrication techniques, particularly to tune the emission spectra and increase emission, have already begun and offer significant promise as an alternative solid-state laser pump source.

REFERENCES

1. W. Streifer, D. R. Scifres, G. L. Harnagel, D. F. Welch, J. Berger, M. Sakamoto, "Advances in Diode Laser Pumps," *IEEE J. Quantum Elect.*, **24** (6), June 1988, pp. 883–894.
2. T. S. Fan, R. L. Byer, "Diode Laser-Pumped Solid-State Lasers," *IEEE J. Quantum Elect.*, **24** (6), June 1988, pp. 895–912.
3. P. Albers, "Diode Pumped Neodymium Lasers," *High-Power Solid-State Lasers and Applications*, C. L. M. Ireland, editor, SPIE Vol. 1277, pp. 48–51, (1990).
4. A. A. Kaminskii, *Laser Crystals: Their Physics and Properties*, (New York: Springer-Verlag, 1981).
5. S. M. Sze, *Physics of Semiconductor Devices*, 2nd. Edition (New York: John Wiley & Sons, 1981), p. 13.
6. L. T. Canham, "Silicon Quantum Wire Array Fabrication by Electrochemical and Chemical Dissolution of Wafers," *Appl. Phys. Lett.*, **57** (10), Sept. 1990, pp. 1046–1048.
7. S. Shih, C. Tsai, K.-H. Li, K. H. Jung, J. C. Campbell, D. L. Kwong, "Control of Porous Si Photoluminescence Through Dry Oxidation," *Appl. Phys. Lett.*, **60** (2), Feb. 1992, pp. 833–835.

8. R. P. Vasquez, R. W. Fathauer, T. George, A. Ksendzov, T. L. Lin, "Electronic Structure of Light-Emitting Porous Si," *Appl. Phys. Lett.*, **60** (8), Feb. 1992, pp. 1004–1006.
9. X. L. Zheng, W. Wang, H. C. Chen, "Anomalous Temperature Dependencies of Photoluminescence for Visible-Light-Emitting Porous Si," *Appl. Phys. Lett.*, **60** (2), Feb. 1992, pp. 986–988.
10. M. S. Brandt, H. D. Fuchs, M. Stutzmann, J. Weber, M. Cardona, "The Origin of Visible Luminescence From 'Porous Silicon': A New Interpretation," *Solid State Commun.*, **81** (4), 1992, pp. 307–312.
11. N. Koshida, H. Koyama, "Visible Electroluminescence from Porous Silicon," *Appl. Phys. Lett.*, **60** (3), Jan. 1992, pp. 347–349.
12. H. P. Maruska, F. Namavar, N. M. Kalkhoran, "Current Injection Mechanism for Porous-Silicon Transparent Surface Light-Emitting Diodes," *Appl. Phys. Lett.*, **61** (11), 14 Sept. 1992, 1338–1340.
13. W. B. Dubbelday, D. M. Szaflarski, R. Shimabukuro, S. D. Russell, M. J. Sailor, "Photoluminescent Thin Film Porous Silicon on Sapphire," *Appl. Phys. Lett.*, **62** (14), Apr. 1993, pp. 1694–1696.
14. J. Sarathy, S. Shih, K. Jung, C. Tsai, K.-H. Li, D.-L. Kwong, J. C. Campbell, S.-L. Yau, A. J. Bard, "Demonstration of Photoluminescence in Nonanodized Silicon," *Appl. Phys. Lett.*, **60** (13), Mar 1992, pp. 1532–1534.
15. R. W. Fathauer, T. George, A. Ksendzov, R. P. Vasquez, "Visible Luminescence From Silicon Wafers Subjected to Stain Etches," *Appl. Phys. Lett.*, **60** (8), Feb. 1992, pp. 995–997.
16. S. K. Ghandi, *VLSI Fabrication Principles*, (New York: Wiley, 1983), pp. 478–482.
17. R. T. Collins, M. A. Tischler, and J. H. Stathis, "Photoinduced Hydrogen Loss From Porous Silicon," *Appl. Phys. Lett.*, **61** (14), Oct. 1992, pp. 1649–1651.
18. C. Tsai, K.-H. Li, J. Sarathy, S. Shih, J. C. Campbell, B. K. Hance, J. M. White, "Thermal Treatment Studies of the Photoluminescence Intensity of Porous Silicon," *Appl. Phys. Lett.*, **59** (22), Nov. 1991, pp. 2814–2816.
19. F. Namavar, H. P. Maruska, N. M. Kalkhoran, "Visible Electroluminescence From Porous Silicon np Heterojunction Diodes," *Appl. Phys. Lett.*, **60** (20), May 1992, pp. 2514–2516.
20. H. Rupprecht, J. M. Woodall, K. Konnerth, D. G. Pettit, "Efficient Electroluminescence From GaAs Diodes at 300K," *Appl. Phys. Lett.*, **9** (6) Sept. 1966, pp. 221–223.

INITIAL DISTRIBUTION

Code 0012	Patent Counsel	(1)
Code 0141	A. Gordon	(1)
Code 50	H. O. Porter	(1)
Code 55	H. E. Rast	(1)
Code 553	G. A. Garcia	(1)
Code 553	R. L. Shimabukuro	(5)
Code 553	W. B. Dubbelday	(5)
Code 553	S. D. Russell	(15)
Code 804	V. N. Smiley	(1)
Code 843	D. A. Gookin	(1)
Code 961	Archive/Stock	(6)
Code 964B	Library	(2)

Defense Technical Information Center
Alexandria, VA 22304-6145 (4)

NCCOSC Washington Liaison Office
Washington, DC 20363-5100

Center for Naval Analyses
Alexandria, VA 22302-0268

Navy Acquisition, Research and Development
Information Center (NARDIC)
Washington, DC 20360-5000

GIDEP Operations Center
Corona, CA 91718-8000

NCCOSC Division Detachment
Warminster, PA 18974-5000

REPORT DOCUMENTATION PAGE

Form Approved
OMB No. 0704-0188

Public reporting burden for this collection of information is estimated to average 1 hour per response, including the time for reviewing instructions, searching existing data sources, gathering and maintaining the data needed, and completing and reviewing the collection of information. Send comments regarding this burden estimate or any other aspect of this collection of information, including suggestions for reducing this burden, to Washington Headquarters Services, Directorate for Information Operations and Reports, 1215 Jefferson Davis Highway, Suite 1204, Arlington, VA 22202-4302, and to the Office of Management and Budget, Paperwork Reduction Project (0704-0188), Washington, DC 20503.

1 AGENCY USE ONLY (Leave blank)	2 REPORT DATE March 1993	3 REPORT TYPE AND DATES COVERED Jun — Sep 1992	
4 TITLE AND SUBTITLE POROUS SILICON FOR PUMPING SOLID-STATE LASERS		5 FUNDING NUMBERS 0601153N 84-CH41 0601152N 953-2W70	
6 AUTHOR(S) S. D. Russell, W. B. Dubbelday, R. L. Shimabukuro		8 PERFORMING ORGANIZATION REPORT NUMBER TD 2461	
7 PERFORMING ORGANIZATION NAME(S) AND ADDRESS(ES) Naval Command, Control and Ocean Surveillance Center (NCCOSC) RDT&E Division San Diego, CA 92152-5001		10 SPONSORING/MONITORING AGENCY REPORT NUMBER	
9 SPONSORING/MONITORING AGENCY NAME(S) AND ADDRESS(ES) Office of Naval Research Arlington, VA 22267-5660		Naval Command, Control and Ocean Surveillance Center (NCCOSC) RDT&E Division Independent Research Program San Diego, CA 92152-5001	
11 SUPPLEMENTARY NOTES			
12a DISTRIBUTION/AVAILABILITY STATEMENT Approved for public release; distribution is unlimited.		12b DISTRIBUTION CODE	
13 ABSTRACT (Maximum 200 words) Preliminary experiments were performed to investigate the feasibility of using silicon-based sources to pump solid-state lasers. Photoluminescent porous silicon and porous silicon-on-sapphire (SOS) have been fabricated using chemical, electrochemical, and photochemical techniques. An electrochemically fabricated porous silicon sample exhibited 5% quantum efficiency when pumped with 5 mW of 457.9 nm argon ion laser light with a peak emission wavelength of 720 nm. This is consistent with other reports that efficiencies between 1 and 10% have been observed. This room temperature performance exceeds the early development of light emission from III-V semiconductors and suggests that continued research and development of the emission mechanism and optimization of the fabrication process can produce, at the very least, functionally equivalent results in a less expensive material which is amenable to large-scale integration.			
14 SUBJECT TERMS porous silicon photoluminescence solid-state lasers laser pumping silicon-on-sapphire		15 NUMBER OF PAGES 20	
17 SECURITY CLASSIFICATION OF REPORT UNCLASSIFIED		16 PRICE CODE	
18 SECURITY CLASSIFICATION OF THIS PAGE UNCLASSIFIED	19 SECURITY CLASSIFICATION OF ABSTRACT UNCLASSIFIED	20 LIMITATION OF ABSTRACT SAME AS REPORT	

UNCLASSIFIED

21a. NAME OF RESPONSIBLE INDIVIDUAL	21b. TELEPHONE <i>(include Area Code)</i>	21c. OFFICE SYMBOL
S. D. Russell	(619) 553-5502	Code 553